

Supplementary File 1: Supplementary experimental section to this study.

Structural characterization

The morphology and crystal structure of the materials were analyzed using a FEI Talos F200S 200 kV field emission transmission electron microscope. The elemental composition and valence distribution of the samples were analyzed using a Thermo ESCALAB 250Xi. The phase structure of the samples was analyzed using an X-ray diffractometer (Rigaku MiniFlex-600) equipped with a Cu-K α radiation X-ray source, with a scanning range of “2 θ = 5° to 80°” and a scanning rate of 10°/min. The orderliness and graphitization of carbon materials were characterized using a LabRAM HR Evolution Raman spectrometer at an excitation wavelength of 532 nm. The specific surface area, porosity, and pore size of the powder samples were measured using an ASAP 2460 specific surface area and porosity analyzer (Micromeritics Instrument Corporation, USA).

Electrochemical measurement

All electrochemical performance tests were conducted using a three-electrode system on a Gamry Interface 1010 electrochemical workstation, with a graphite rod as the working electrode and a mercury/mercury oxide electrode as the reference electrode. First, 4 mg of catalyst was uniformly dispersed in 200 μ L of 0.5% Nafion solution, followed by ultrasonic treatment to ensure uniform dispersion. Subsequently, 50 μ L of the uniformly formed ink was coated onto the surface of carbon paper using an electrode holder. The carbon paper was used as the working electrode, with a catalyst loading of approximately 2 mg/cm².

The CV curve was measured at room temperature using linear sweep voltammetry (LSV) and cyclic voltammetry (CV) in a three-electrode system to improve the wettability of carbon paper in the electrolyte and activate the carbon layer surface. All tests used 1 mol/L KOH as the electrolyte, and the test data were not iR-corrected. All potentials were calculated based on the reversible hydrogen electrode (RHE) using the following formula:

$$E(vs.RHE)=E(vs.Hg/HgO)+0.098+0.0591\times pH$$

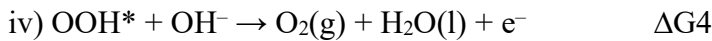
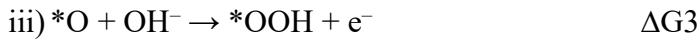
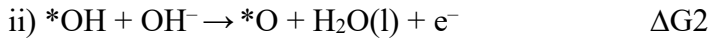
Electrochemical impedance spectroscopy (EIS) was measured in the frequency range of 100 kHz to 10 mHz at an overpotential of 250 mV. The electrocatalytic activity was plotted after iR reduction correction of the entire system. The electrochemical surface area (ECSA) was calculated by measuring cyclic voltammetry (CV) at different scan rates and plotting the capacitance current scan rate curve.

DFT calculation method

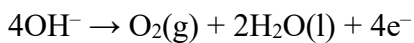
All calculations were performed using the plane-wave density functional theory (DFT) method as implemented in the Vienna Atomic Structure Package (VASP) [1,2]. The exchange-correlation functional employed the generalized gradient approximation (GGA) as implemented in the Perdew-Burke-Ernzerhof functional [3]. The projected augmented wave (PAW) method was used to handle the interactions between valence electrons and core electrons [4]. A sufficient vacuum zone of 18 Å was adopted in the z direction to

avoid periodic interactions. During the geometric relaxation process, a cutoff energy of 500 eV was selected. In the structural optimization process, the Brillouin zone sampling used a $2 \times 2 \times 1$ k-point grid centered at gamma, while the electronic structure calculations employed a more dense $8 \times 8 \times 1$ grid. The convergence criteria for force and energy were set to 0.02 eV/Å and 1×10^{-5} eV, respectively.

The OER reaction for four-electron pathway in alkaline electrolyte:



Overall reaction:



*Denotes the adsorbed state, (l) and (g) denote the liquid phase and gas phase, respectively.

The Gibbs free energy change (ΔG) is defined as:

$$\Delta\text{G} = \Delta\text{E} + \Delta\text{ZPE} - T\Delta\text{S} + \Delta\text{GU} + \Delta\text{GpH}$$

where, ΔE , ΔZPE , and ΔS are the adsorption energy, zero-point energy correction, and entropy change, respectively, calculated using density functional theory. T , ΔGU , and ΔGpH are the temperature caused by the applied electrode potential, the free energy correction caused by the solvent pH, and the free energy change caused by the applied electrode potential, respectively.

References

- [1] Kresse G, Furthmüller J. 1996. Efficiency of ab-initio total energy calculations for metals and semiconductors using a plane-wave basis set. *Computation Mater Science* 6:15–50 [https://doi.org/10.1016/0927-0256\(96\)00008-0](https://doi.org/10.1016/0927-0256(96)00008-0).
- [2] Kresse G, Furthmüller J. 1996. Efficient iterative schemes for ab initio total-energy calculations using a plane-wave basis set. *Physical Review B* 54:11169–11186 <https://doi.org/10.1103/PhysRevB.54.11169>
- [3] Perdew JP, Burke K, Ernzerhof M. 1996. Generalized Gradient Approximation Made Simple. *Physical Review Letters* 77:3865–3868 <https://doi.org/10.1103/PhysRevLett.77.3865>
- [4] Blochl PE. 1994. Projector augmented-wave method. *Physical Review B*. 50:17953–17979 <https://doi.org/10.1103/PhysRevB.50.17953>